

***M1* and Gamow-Teller transitions in $T=1/2$ nuclei ^{23}Na and ^{23}Mg**

Y. Fujita,^{1,*} Y. Shimbara,¹ I. Hamamoto,² T. Adachi,¹ G. P. A. Berg,³ H. Fujimura,³ H. Fujita,¹ J. Görres,⁴ K. Hara,³ K. Hatanaka,³ J. Kamiya,³ T. Kawabata,³ Y. Kitamura,³ Y. Shimizu,³ M. Uchida,⁵ H. P. Yoshida,³ M. Yoshifuku,¹ and M. Yosoi⁵

¹*Department of Physics, Osaka University, Toyonaka, Osaka 560-0043, Japan*

²*Division of Mathematical Physics, LTH, University of Lund, P.O. Box 118, S-22100 Lund, Sweden*

³*Research Center for Nuclear Physics, Osaka University, Ibaraki, Osaka 567-0047, Japan*

⁴*Department of Physics, University of Notre Dame, Notre Dame, Indiana 46556*

⁵*Department of Physics, Kyoto University, Kyoto 606-8502, Japan*

(Received 3 August 2002; published 29 October 2002)

The magnetic dipole ($M1$) operator consists not only of the usually dominant isovector (IV) spin ($\sigma\tau$) term, but also of IV orbital ($l\tau$), isoscalar (IS) spin (σ), and IS orbital (l) terms. On the other hand, the Gamow-Teller (GT) operator contains only the $\sigma\tau$ term. Under the assumption that isospin is a good quantum number, isobaric analog structure is expected in a pair of $T=1/2$ mirror nuclei, and thus analogous transitions are found. For the $M1$ transitions in the $T=1/2$ mirror nuclei pair ^{23}Na - ^{23}Mg , the contributions of these various terms have been studied by comparing the strengths of the analogous $M1$ γ transitions and the GT transitions deduced from high-resolution $^{23}\text{Na}(^3\text{He},t)^{23}\text{Mg}$ charge-exchange measurements. In some $M1$ transitions, unusually large orbital contributions were observed even for strong transitions, while in some others, almost no orbital contribution was found. It is known that ^{23}Na and ^{23}Mg are deformed. The large difference of the orbital contributions is explained based on the different selection rules for l and σ operators in transitions connecting different deformed bands. Precise excitation energies are determined for the states above the proton separation energy in ^{23}Mg . These states are of astrophysical interest because of their important role played in the $^{22}\text{Na}(p,\gamma)^{23}\text{Mg}$ reaction of the Ne-Na cycle in nucleosynthesis.

DOI: 10.1103/PhysRevC.66.044313

PACS number(s): 25.55.Kr, 21.10.Re, 23.20.Lv, 27.30.+t

I. INTRODUCTION

The magnetic dipole ($M1$) operator for $M1$ γ transitions and the Gamow-Teller (GT) operator for GT β decays are similar in that they have the same major component, i.e., the isovector (IV) spin ($\sigma\tau$) term, although transitions originate from the electromagnetic and weak interactions, respectively [1–3]. The difference between them is that the electromagnetic $M1$ operator contains not only the $\sigma\tau$ term, but also IV orbital ($l\tau$), isoscalar (IS) spin (σ), and IS orbital (l) terms.

Assuming that isospin T is a good quantum number, isospin multiplet states are found in nuclei with the same mass number A but different isospin z -component defined by $T_z = (N-Z)/2$. If charge symmetry of the nuclear interaction is assumed, then for every state in one of the isospin $T=1/2$, odd- A mirror nuclei, an analog state with almost identical structure should be found at the corresponding excitation energy in the partner nucleus. Because of the identical nature of the analog states, the $M1$ and GT transitions from the ground states to a pair of analog states can be directly compared in terms of matrix elements. The similarity and/or difference of strengths of these analogous $M1$ and GT transitions will show the microscopic nature of the $M1$ transitions [4], namely, (1) the IS and IV contributions, and (2) the orbital and spin contributions in individual $M1$ transitions.

In the sd -shell region most of the $T_z=1/2$ nuclei are stable, while the ground states of $T_z=-1/2$ nuclei are un-

stable due to Coulomb energy. They undergo β^+ decay to excited states of the $T_z=1/2$ mirror partner mainly through GT transitions. The GT transition strengths $B(\text{GT})$ are obtained from decay studies, but the accessible range of excitation energy (E_x) is limited by the Q value.

These β^+ decays are analogous to the transitions studied in the (p,n) -type charge-exchange (CE) reactions on $T_z=1/2$ target nuclei. In CE reactions, like (p,n) or $(^3\text{He},t)$, at intermediate energies (>100 MeV/nucleon), it has been found that the 0° cross sections are proportional to the $B(\text{GT})$ values from β -decay studies [5,6]. Therefore, CE reactions have been used extensively to map the GT strengths over a wide excitation-energy range overcoming the “ Q -value limitation” of β decays [7].

The most direct information on $B(M1)$ values is obtained from $M1$ γ decays. The (e,e') reactions at backward angles are also important in studying $B(M1)$ values for the highly excited states.

Contributions from spin and orbital terms in $M1$ transitions were first studied for the $\Delta T=1$, IV $M1$ transitions starting from the ground state of $T=0$ even-even target nuclei, in which no IS contribution is expected. The contributions were studied for the ^{32}S target by comparing (p,n) and (e,e') reactions [8] and for ^{28}Si and ^{24}Mg targets by comparing $(^3\text{He},t)$ and (e,e') reactions [9–11]. Since the ground state of mirror nuclei are $T=1/2$, the IS term can also contribute to $T=1/2 \rightarrow 1/2$ $M1$ transitions.

For the study of these contributions, a transition-by-transition comparison of strengths from electromagnetic measurements and CE reactions is essential. In order to make

*Email address: fujita@rcnp.osaka-u.ac.jp

a reliable comparison, a good energy resolution is required especially in CE reactions. The advantage of the (${}^3\text{He}, t$) reaction is the possibility of achieving high resolution of around 50 keV even at intermediate incident energies by using a magnetic spectrometer for the analysis of outgoing tritons [12]. The combined IS and orbital contributions were studied for the ${}^{27}\text{Al}$ - ${}^{27}\text{Si}$ mirror nuclei [13] by comparing $B(M1)$ values from a study of γ decay in ${}^{27}\text{Al}$ with the $B(\text{GT})$ values from a good-resolution ${}^{27}\text{Al}({}^3\text{He}, t)$ reaction. In addition, the IS and orbital contributions were separated by further using $B(M1)$ information on the mirror γ decays in ${}^{27}\text{Si}$ [4].

In this paper, we compare the analogous transitions in the pair of mirror nuclei ${}^{23}\text{Na}$ and ${}^{23}\text{Mg}$. It is well known that the nuclei in the $A=23$ region are strongly deformed. The interest is to unveil the microscopic structure of each $M1$ transition in deformed nuclei, i.e., to see how the deformation affects the IS/IV and orbital/spin contributions in various $M1$ transitions. Using the γ -decay data in ${}^{23}\text{Na}$, $B(M1)$ values of the transitions to the ground state are calculated for the states up to the proton separation energy. In addition, $B(M1)$ values are calculated for a few excited states in ${}^{23}\text{Mg}$. The $B(\text{GT})$ values are obtained by using the ${}^{23}\text{Na}({}^3\text{He}, t){}^{23}\text{Mg}$ reaction performed at 0° . Contributions of IS and IV terms as well as spin and orbital terms in $M1$ transitions are studied by comparing the $B(M1)$ values with those of the $B(\text{GT})$ values from analogous transitions.

Owing to the high resolution achieved in the present work, level energies of excited states were accurately determined. The states just above the proton threshold in ${}^{23}\text{Mg}$ are of astrophysical interest. The obtained excitation energies of these states are compared with previous works.

II. $M1$ AND GT TRANSITIONS IN DEFORMED MIRROR NUCLEI

We summarize the characteristics of analogous $M1$ and GT transitions in odd- A mirror nuclei referring to the formalism given in Refs. [4] and [13]. In odd- A deformed nuclei, we separate the degree of freedom of the odd particle from that of the core, which makes collective rotation.

A. Analogous $M1$ and GT transitions

The $M1$ operator in the particle-rotor model is given by [see Eq. (4A-11) of Ref. [14]]

$$\begin{aligned} \mathcal{M}(1)_\mu &= \sqrt{\frac{3}{4\pi}} \mu_N (g_R R_\mu + g_\ell \ell_\mu + g_s s_\mu) \\ &= \sqrt{\frac{3}{4\pi}} \mu_N [g_R J_\mu + (g_\ell - g_R) \ell_\mu + (g_s - g_R) s_\mu], \end{aligned} \quad (1)$$

where μ_N is the nuclear magneton and $\mu = -1, 0, \text{ and } +1$. The angular momentum and the gyromagnetic factor (g factor) of the rotor (core) are expressed by \mathbf{R} and g_R , while the orbital and spin g factors of the particle are represented by g_ℓ and g_s , respectively. Assuming a uniform rotation of a

charged body, $g_R \approx Z/A$ is expected [14]. The total angular momentum is denoted by \mathbf{J} , and the angular momentum and spin of the odd particle by ℓ and s , respectively, where the relationship

$$\mathbf{J} = \mathbf{R} + \ell + s \quad (3)$$

holds. Since \mathbf{J} is a good quantum number, only the last two terms in Eq. (2) contribute to the $M1$ transitions. By introducing the isospin operator, whose z component τ_z is $+1$ and -1 for a neutron and proton, respectively, we get

$$(g_\ell - g_R) \ell_\mu = \left[\left(\frac{1}{2} (g_\ell^\pi + g_\ell^\nu) - g_R \right) - \frac{1}{2} (g_\ell^\pi - g_\ell^\nu) \tau_z \right] \ell_\mu \quad (4)$$

$$= (g_l^{\text{IS}} - g_l^{\text{IV}} \tau_z) \ell_\mu, \quad (5)$$

and

$$(g_s - g_R) s_\mu = \left[\left(\frac{1}{2} (g_s^\pi + g_s^\nu) - g_R \right) - \frac{1}{2} (g_s^\pi - g_s^\nu) \tau_z \right] s_\mu \quad (6)$$

$$= (g_s^{\text{IS}} - g_s^{\text{IV}} \tau_z) s_\mu, \quad (7)$$

where the IS and IV combinations of g factors are expressed by the coefficients g^{IS} and g^{IV} . Using the bare orbital and spin g factors of protons and neutrons, i.e., $g_\ell^\pi = 1$ and $g_\ell^\nu = 0$, and $g_s^\pi = 5.586$ and $g_s^\nu = -3.826$, we get $g_\ell^{\text{IS}} = 0.5 - g_R$ and $g_s^{\text{IS}} = 0.880 - g_R$, and $g_\ell^{\text{IV}} = 0.5$ and $g_s^{\text{IV}} = 4.706$, respectively.

By using the relationship $s_\mu = (1/2)\sigma_\mu$ and $\tau_z = \tau_0$, and applying the Wigner-Eckart theorem in the spin and isospin spaces, the reduced $M1$ transition strength $B(M1)$ is expressed as

$$\begin{aligned} B(M1) &= \frac{1}{2J_i+1} \frac{3}{4\pi} \mu_N^2 \left[\left(g_\ell^{\text{IS}} M_{M1}(\ell) + g_s^{\text{IS}} \frac{1}{2} M_{M1}(\sigma) \right) \right. \\ &\quad \left. - \frac{C_{M1}}{\sqrt{2T_f+1}} \left(g_\ell^{\text{IV}} M_{M1}(\ell\tau) + g_s^{\text{IV}} \frac{1}{2} M_{M1}(\sigma\tau) \right) \right]^2 \end{aligned} \quad (8)$$

$$= \frac{1}{2J_i+1} \frac{3}{4\pi} \mu_N^2 \left[M_{M1}^{\text{IS}} - \frac{C_{M1}}{\sqrt{2T_f+1}} M_{M1}^{\text{IV}} \right]^2, \quad (9)$$

where C_{M1} expresses the isospin Clebsch-Gordan (CG) coefficient ($T_i T_{z_i} 10 | T_f T_{z_f}$), where $T_{z_f} = T_{z_i}$ holds. The matrix elements are $M_{M1}(\ell) = \langle J_f T_f | \ell | J_i T_i \rangle$ and $M_{M1}(\sigma) = \langle J_f T_f | \boldsymbol{\sigma} | J_i T_i \rangle$ for the IS part, and $M_{M1}(\ell\tau) = \langle J_f T_f | \ell \boldsymbol{\tau} | J_i T_i \rangle$ and $M_{M1}(\sigma\tau) = \langle J_f T_f | \boldsymbol{\sigma} \boldsymbol{\tau} | J_i T_i \rangle$ for the IV part. Owing to the large value of the coefficient g_s^{IV} , the IV spin term, i.e., $(1/2)g_s^{\text{IV}} M_{M1}(\sigma\tau)$, is usually the largest [1,2]. The IS term M_{M1}^{IS} is usually much smaller than the IV term M_{M1}^{IV} . The IS term can interfere destructively or constructively with the IV term. In addition, the IV orbital term can interfere with the IV spin term.

A GT transition is caused by the $\sigma\tau$ operator. The one-body operator for GT transitions is

$$\mathcal{G}_{\pm} \equiv \sigma\tau_{\pm} = \mp \frac{1}{\sqrt{2}} \sigma\tau_{\pm 1}. \quad (10)$$

Its reduced strength in isospin is given by [4]

$$B(\text{GT}) = \frac{1}{2J_i+1} \frac{1}{2} \frac{C_{\text{GT}}^2}{2T_f+1} [M_{\text{GT}}(\sigma\tau)]^2, \quad (11)$$

where C_{GT} expresses the isospin CG coefficient ($T_i T_{z_i} 1 \pm 1 | T_f T_{z_f}$), and $T_{z_f} = T_{z_i} \pm 1$. The matrix element $M_{\text{GT}}(\sigma\tau)$ denotes the (IV spin type) GT transition matrix element, just like the $\sigma\tau$ matrix element in the $M1$ transition. The magnitude, however, is slightly different, as explained in the next paragraph.

It is known that the $\sigma\tau$ terms of the $M1$ operator and GT operator are both reduced. The reduction is partly attributed to the core polarization [14] and partly to the so-called meson exchange currents (MEC). The core polarization modifies the initial and final wave functions, and thus the effect on the analogous $M1$ and GT would be the same in the $N=Z$ case. On the other hand, the MEC effect can be different, because the $M1$ operator has τ_0 nature, while the GT operator has τ_{\pm} nature. The different contributions of the MEC to the $M1$ and GT operators have been studied theoretically [15,16] and experimentally [9,10,13,17–19]. These effects are expressed by the ratio

$$R_{\text{MEC}} = [M_{M1}(\sigma\tau)]^2 / [M_{\text{GT}}(\sigma\tau)]^2. \quad (12)$$

The most probable value $R_{\text{MEC}} = 1.25$ is deduced for nuclei in the middle of sd shell [4].

Under the assumption that isospin is a good quantum number, a very similar structure is expected for the analog states in a pair of $T_z = \pm 1/2$ mirror nuclei. Therefore almost the same $B(\text{GT})$ values are expected for the mirror GT transitions that can be studied in the β decay and the CE reaction starting from the ground states of $T_z = -1/2$ and $+1/2$ nuclei, respectively. In the comparison of the GT transitions with the analogous $M1$ transitions, a simple relationship is obtained for the transition strengths if the $\sigma\tau$ term is dominant in the $M1$ transition. From the comparison of Eq. (8) and Eq. (11), the ‘‘quasiproportionality’’ between $B(\text{GT})$ and $B(M1)$ is expressed as

$$B(M1) \approx \frac{3}{8\pi} (g_s^{\text{IV}})^2 \mu_N^2 \frac{C_{M1}^2}{C_{\text{GT}}^2} R_{\text{MEC}} B(\text{GT}) \quad (13)$$

$$= 2.644 \mu_N^2 \frac{C_{M1}^2}{C_{\text{GT}}^2} R_{\text{MEC}} B(\text{GT}). \quad (14)$$

For a transition from a $T_i = 1/2$ state to a $T_f = 1/2$ state in mirror nuclei, the ratio of squared CG coefficients is $1/2$, while the ratio is 2 when the transition is from a $T_i = 1/2$ state to a $T_f = 3/2$ state.

Our aim is to compare the $M1$ and GT transition strengths for the analogous transitions. From Eq. (14), we find that renormalized $B(M1)$ values defined by

$$B^R(M1) = \begin{cases} \frac{2}{2.644 \mu_N^2} B(M1) & \text{for } T_f = 1/2 \\ \frac{1}{2 \times 2.644 \mu_N^2} B(M1) & \text{for } T_f = 3/2 \end{cases} \quad (15)$$

can be compared directly with the values of $B(\text{GT})$.

B. IS and orbital contributions to $M1$ transitions

In order to examine the interference of IS and IV orbital terms with the IV spin term in an $M1$ transition, we define the following ratio, taking effects of the MEC [Eq. (12)] into consideration [13]:

$$R_{\text{ISO}} = \frac{1}{R_{\text{MEC}}} \frac{B^R(M1)}{B(\text{GT})}. \quad (17)$$

By comparing Eq. (8) and Eq. (11), it is seen that $R_{\text{ISO}} > 1$ usually shows that the IS term and/or the IV orbital term make a constructive contribution to the IV spin term, while $R_{\text{ISO}} < 1$ shows a destructive contribution. As discussed in Ref. [4] and as will be discussed later, the contribution of the IS term is minor. Therefore, it is expected that the deviation of R_{ISO} from unity mainly shows a contribution of the IV orbital term in each $M1$ transition.

Under the assumption that the IS term is small, IS and IV contributions can be separated if $B(M1)$ values are known for a pair of analogous transitions in $T_z = \pm 1/2$ mirror nuclei. In these transitions, the isospin CG coefficients C_{M1} have opposite signs, and Eq. (9) can be rewritten as

$$B(M1)_{\pm} = \frac{1}{2J_i+1} \frac{3}{4\pi} \mu_N^2 \left[M_{M1}^{\text{IS}} \mp \frac{|C_{M1}|}{\sqrt{2T_f+1}} M_{M1}^{\text{IV}} \right]^2 \quad (18)$$

for the transitions in $T_z = \pm(1/2)$ nuclei. Therefore $B_{\text{IS}}(M1)$ and $B_{\text{IV}}(M1)$, which are defined by

$$B_{\text{IS}}(M1) = \frac{1}{2J_i+1} \frac{3}{4\pi} \mu_N^2 [M_{M1}^{\text{IS}}]^2 \quad (19)$$

and

$$B_{\text{IV}}(M1) = \frac{1}{2J_i+1} \frac{3}{4\pi} \mu_N^2 \frac{C_{M1}^2}{2T_f+1} [M_{M1}^{\text{IV}}]^2, \quad (20)$$

respectively, are separately obtained by solving the pair of Eqs. (18) as simultaneous equations. The $B_{\text{IV}}(M1)$ is expressed by using the $B(M1)_{\pm}$ values

$$B_{\text{IV}}(M1) = \frac{1}{4} [\sqrt{B(M1)_{+}} + \sqrt{B(M1)_{-}}]^2, \quad (21)$$

while the $B_{\text{IS}}(M1)$ is given by

$$B_{\text{IS}}(M1) = \frac{1}{4} [\sqrt{B(M1)_+} - \sqrt{B(M1)_-}]^2. \quad (22)$$

By defining the ratio

$$R_{\text{IS}} = \frac{B(M1)}{B_{\text{IV}}(M1)}, \quad (23)$$

the contribution of the IS term can be examined. If the IS contribution is constructive (destructive) in a specific $M1$ transition, then the ratio is larger (smaller) than unity.

Once IS and IV terms are separated, the orbital contribution to the IV term is evaluated in a similar way as the combined IS and orbital contribution was evaluated by the ratio R_{ISO} . Replacing $B^R(M1)$ in Eq. (17) by $B_{\text{IV}}^R(M1)$, which is defined similarly to $B^R(M1)$ in Eq. (15) or Eq. (16), we introduce the ratio

$$R_{\text{OC}} = \frac{1}{R_{\text{MEC}}} \frac{B_{\text{IV}}^R(M1)}{B(\text{GT})}. \quad (24)$$

The ratio is usually larger (smaller) than unity if the IV orbital contribution is constructive (destructive) to the IV spin term in the IV part of a specific $M1$ transition.

A similar argument is possible for the magnetic moments of the analogous states in $T_z = \pm 1/2$ nuclei (for details, see Ref. [4]). The magnetic moment μ of a state with spin J and isospin T is defined by

$$\mu = \langle JTT_z | \mathcal{M}(1)_z | JTT_z \rangle. \quad (25)$$

By applying the Wigner-Eckart theorem in the spin and isospin space, we get

$$\mu = \frac{\sqrt{J}}{\sqrt{(J+1)(2J+1)}} \mu_N \left[M_{M1}^{\text{IS}} - \frac{C_{M1}}{\sqrt{2T+1}} M_{M1}^{\text{IV}} \right], \quad (26)$$

where the IS and IV matrix elements are the same as those in Eq. (9), except that the initial and final states are the same. The CG coefficient is $C_{M1} = (TT_z 10 | TT_z)$. Again it has opposite sign in the magnetic moments μ_{\pm} of the $T_z = \pm 1/2$ nuclei.

The IS and IV moments defined by $\mu_{\text{IS}} = \frac{1}{2}(\mu_+ + \mu_-)$ and $\mu_{\text{IV}} = \frac{1}{2}(\mu_+ - \mu_-)$, respectively, can be related to the IS and IV $M1$ matrix elements

$$\mu_{\text{IS}} = \frac{\sqrt{J}}{\sqrt{(J+1)(2J+1)}} \mu_N M_{M1}^{\text{IS}} \quad (27)$$

and

$$\mu_{\text{IV}} = \frac{\sqrt{J}}{\sqrt{(J+1)(2J+1)}} \mu_N \frac{-|C_{M1}|}{\sqrt{2T+1}} M_{M1}^{\text{IV}}. \quad (28)$$

The constructive or destructive contributions of the IS term of the magnetic moments are expressed by introducing the ratio

$$R_{\text{IS}} = \left(\frac{\mu}{\mu_{\text{IV}}} \right)^2. \quad (29)$$

The ratio R_{OC} can also be defined for the magnetic moments. As discussed in Ref. [4], the ratio corresponding to Eq. (24) is given by

$$R_{\text{OC}} = \frac{1}{R_{\text{MEC}}} \frac{2(J+1)}{J(g_s^{\text{IV}})^2 \mu_N^2} \frac{C_{\text{GT}}^2}{C_{M1}^2} \frac{\mu_{\text{IV}}^2}{B(\text{GT})}, \quad (30)$$

We use the above formulas (29) and (30) for the pair of magnetic moments of ground states, where the ratio C_{M1}^2/C_{GT}^2 is 1/2.

III. EXPERIMENT

At intermediate energies (≥ 100 MeV/nucleon) and at forward angles including 0° , GT states become prominent in ($^3\text{He}, t$) reactions, because of their $L=0$ nature and the dominance of the $\sigma\tau$ part of the effective nuclear interaction [20,21]. In order to study the transitions to the GT states in ^{23}Mg , a $^{23}\text{Na}(^3\text{He}, t)$ experiment was performed at the Research Center for Nuclear Physics (RCNP), Osaka by using a 140 MeV/nucleon ^3He beam from the $K=400$, RCNP Ring Cyclotron and the Grand Raiden spectrometer [22] placed at 0° .

The target was a thin foil of Na_2CO_3 using polyvinyl alcohol as supporting material [23]. The total thickness of the target was approximately 2 mg/cm^2 . The target is effectively a mixture of ^{23}Na , carbon isotopes ^{12}C and ^{13}C (natural abundance 98.9% and 1.1%, respectively), and oxygen isotopes ^{16}O and ^{18}O (natural abundance 99.8% and 0.2%, respectively). After the ($^3\text{He}, t$) charge-exchange reactions, these nuclei become ^{23}Mg , ^{12}N , ^{13}N , ^{16}F , and ^{18}F . The reaction Q values of them are $-4.08, -17.36, -2.24, -15.44$, and -1.67 MeV, respectively. Owing to the large difference of Q values, the low-lying states in ^{23}Mg are observed without being affected by the strongly excited states in ^{12}N and ^{16}F . Since the Q values of ^{13}C and ^{18}O nuclei are smaller than that of ^{23}Na , ground and excited states of ^{13}N and ^{18}F may disturb the ^{23}Mg spectrum. The identification of these states and the states of ^{23}Mg was possible due to the high resolution of this experiment as will be described below.

The outgoing tritons within the full acceptance of the spectrometer [$\approx \pm 20$ mrad and $\approx \pm 40$ mrad in horizontal (x) and vertical (y) directions, respectively] were momentum analyzed and detected at the focal plane with a multiwire drift-chamber system allowing track reconstruction [24]. The acceptance of the spectrometer was subdivided in the software analysis by using raytrace information.

A resolution far better than the momentum spread of the beam was realized by applying the *dispersion matching* technique [25]. Using the new high-resolution ‘‘WS’’ course [26] for the beam transportation and the ‘‘faint beam method’’ to diagnose the matching conditions [27,28], an energy resolution of 45 keV [full width at half maximum (FWHM)] was achieved. With the improvement of resolution, states of ^{23}Mg up to $E_x = 11$ MeV were clearly resolved as shown in Fig. 1.

In accurately determining the scattering angle Θ near 0° , scattering angles in both the x direction (θ) and y direction (ϕ) should be measured equally well, where Θ is defined by

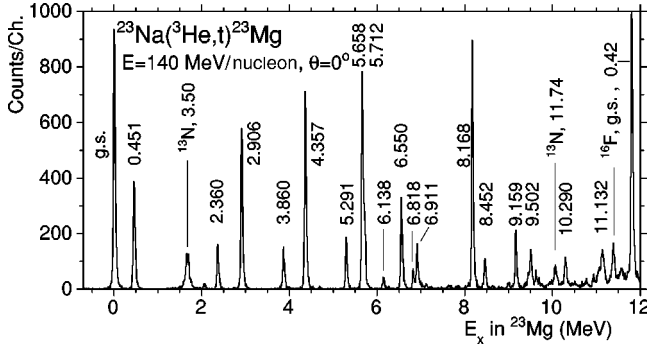


FIG. 1. The $^{23}\text{Na}(^3\text{He},t)^{23}\text{Mg}$ spectrum measured at 0° by using a thin Na_2CO_3 target. A high resolution of 45 keV has been achieved. The states listed in Table I are indicated by their excitation energies. The 3.50 MeV state in ^{13}N is also indicated. For other details, see text.

$\sqrt{\theta^2 + \phi^2}$. Good θ resolution was achieved by applying the *angular dispersion matching* technique [25], while that of ϕ by realizing the “overfocus mode” in the spectrometer [29]. The “ 0° spectrum” in Fig. 1 shows events for the scattering angles $\Theta \leq 0.8^\circ$.

In order to identify the states originating from carbon and oxygen isotopes, a spectrum of a Mylar target was measured under the same condition as for the Na_2CO_3 target. From a comparison of both spectra, it was found that the peak at $E_x \approx 1.7$ MeV in Fig. 1 was the 3.50 MeV state of ^{13}N , and the peak at ≈ 10.1 MeV was partly the ^{13}N , 11.74 MeV state [30]. It was also found that the small tail in the right side of the 6.91 MeV state was the 8.92 MeV state of ^{13}N . The peaks at $E_x \approx 11.4$ MeV and 11.8 MeV were identified as the ground and the 0.42 MeV states in ^{16}F . The ^{18}F ground state ($J^\pi = 1^+$) was also observed, but it is outside the energy range of the spectrum due to the small Q value of the reaction.

An accurate E_x value with an error of less than 1 keV is known for the 0.451 MeV state of ^{23}Mg [31], but errors given for higher excited states are larger (see Table I). The E_x values of other excited states observed here were determined with the help of kinematic calculations. Known states of ^{13}N [32] and ^{16}F [33], which were observed in the spectrum of Mylar target, and the ^{26}Al states, which were observed in the $^{26}\text{Mg}(^3\text{He},t)^{26}\text{Al}$ spectrum taken under the same condition as for the Na_2CO_3 target, were used as calibration standard. Owing to the small Q value of the ($^3\text{He},t$)

TABLE I. The GT transition strengths $B(\text{GT})$ from $^{23}\text{Mg} \rightarrow ^{23}\text{Na}$ β decay and $^{23}\text{Na}(^3\text{He},t)^{23}\text{Mg}$ reaction. Mirror symmetry of transition strengths is assumed in deriving the latter from the former. For details of the derivation, see text. Excitation energies are given in units of MeV, and their errors are given in units of keV in parentheses.

States in ^{23}Na			States in ^{23}Mg			
E_x^b	$2J^\pi^b$	β decay $B(\text{GT})^b$	E_x^b	$2J^\pi^b$	E_x	$(^3\text{He},t)^a$ $B(\text{GT})$
0.0	3^+	0.190 ± 0.004	0.0	3^+	0.0	$(0.340 \pm 0.014)^c$
0.440	5^+	0.146 ± 0.006^d	0.451	5^+	0.451	0.146 ± 0.006^d
2.391	1^+	0.043 ± 0.006	2.359(2)	1^+	2.360(3)	0.055 ± 0.004
			2.908(3)	$(3,5)^+$	2.906(3)	0.193 ± 0.011
			3.864(4)	$(3,5)^+$	3.860(3)	0.055 ± 0.004
			4.354(4)	1^+	4.357(3)	0.250 ± 0.013
			5.287(4)	$(3,5)^+$	5.291(3)	0.066 ± 0.005
			5.656(6)	5^+	5.658(4)	0.270 ± 0.017^e
			5.691(6)	$(1-9)^+$		
			5.711(6)	$(1-9)^+$	5.712(8)	0.061 ± 0.009^e
			6.125(5)	$(1-11)^-$	6.138(3)	
			6.538(5)	$(1-9)^+$	6.550(3)	0.116 ± 0.007
			6.810(5)		6.818(3)	0.028 ± 0.003
			6.899(4)	5^+	6.911(3)	0.057 ± 0.004
			8.166(2)	5^+	8.168(4)	0.290 ± 0.015
			8.455(4)	$(3-13)^+$	8.452(5)	0.039 ± 0.003
			[9.138(6)]	$(3-13)^+$	9.159(6)	0.069 ± 0.005
			[9.465(6)]	$(1-9)^+$	9.502(6)	0.055 ± 0.004
					10.290(7)	0.046 ± 0.004
					11.132(8)	0.062 ± 0.005

^aPresent work.

^bFrom Ref. [31].

^cIncluding Fermi-transition strength. See text for details.

^d $B(\text{GT})$ value used for the calibration of ($^3\text{He},t$) values.

^eClose doublet states.

reaction on ^{13}C and the large Q value on ^{16}O , all E_x values of ^{23}Mg states were determined by interpolation. In addition, since the Q value of the $(^3\text{He},t)$ reaction on ^{26}Mg ($Q = -4.02$ MeV) is similar to that on ^{23}Na ($Q = -4.08$ MeV) and accurate E_x values of ^{26}Al states are known up to $E_x = 7.8$ MeV, E_x values of states up to 8 MeV in ^{23}Mg were determined especially with good accuracy. The excitation energies from Ref. [31] and those determined in the present work are listed in columns 4 and 6 of Table I, respectively.

The intensities of individual peaks were obtained by applying a peak-decomposition program using the shape of the well separated peak at 4.357 MeV. The 5.658 and 5.712 MeV states were observed as an unresolved doublet, where the latter is observed as a shoulder. Since a 5.691 MeV state with $J^\pi = (1-9)^+$ is listed in Ref. [31], a peak decomposition including this peak was also applied. The result, however, showed that the observed peak shape was well reproduced by the two peaks at 5.658 and 5.712 MeV.

Owing to the *angular dispersion matching* and also to the overfocus mode of the spectrometer setting, it is estimated that an angle resolution of better than 8 mrad was achieved [29]. In order to identify the $L=0$ nature of states, relative intensities of peaks were examined for the spectra with the angle cuts $\Theta = 0^\circ - 0.5^\circ$, $0.5^\circ - 1.0^\circ$, $1.0^\circ - 1.5^\circ$, and $1.5^\circ - 2.0^\circ$. It was found that all states, except the 6.138 MeV state, listed in Table I showed a similar relative decrease of their strengths with increasing Θ . We judge that transitions to all of these states, except that to the 6.138 MeV state, are of $L=0$ nature.

According to Ref. [31], a state having a similar excitation energy with the 6.138 MeV state is at 6.125 MeV. Possible spin values $2J=1-11$ and negative parity are assigned to this state. Clear observation at 0° suggests that the 6.138 MeV state is populated with small L transfer.

IV. DATA ANALYSIS

A. $B(\text{GT})$ evaluation from β -decay data

The ^{23}Mg nucleus has a Q_{EC} value of 4.0583 ± 0.0013 MeV. Using the half-life of 11.317 ± 0.011 s and branching ratios to the ground state and two excited states of ^{23}Na compiled in Ref. [31], the partial half-lives t were calculated. The $B(\text{GT})$ values were obtained by using the relationship [34]

$$B(\text{F})(1 - \delta_C) + \left[\frac{g_A}{g_V} \right]^2 B(\text{GT}) = \frac{6145 \pm 4}{f(1 + \delta_R)t}. \quad (31)$$

The f values including the radiative correction $(1 + \delta_R)$ were calculated using the tables of Wilkinson and Macefield [35]. The $B(\text{GT})$ values calculated by using the ratio $(g_A/g_V) = 1.266 \pm 0.004$ [34,36] are listed in column 3 of Table I. For the ground state transition, both GT and Fermi transitions contribute. The $B(\text{GT})$ value for this transition was calculated assuming the reduced Fermi transition strength $B(\text{F}) = 1$ and the Coulomb correction term $(1 - \delta_C) = 0.997$.

B. $B(\text{GT})$ evaluation from $(^3\text{He},t)$ data

It is known that at 0° the CE cross section for a GT transition is approximately proportional to $B(\text{GT})$ [5,6,37],

$$\frac{d\sigma_{\text{CE}}}{d\Omega}(0^\circ) \approx K N_{\sigma\tau} |J_{\sigma\tau}(0)|^2 B(\text{GT}), \quad (32)$$

where $J_{\sigma\tau}(0)$ is the volume integral of the effective interaction $V_{\sigma\tau}$ at momentum transfer $q=0$, K is the kinematic factor, $N_{\sigma\tau}$ is a distortion factor. In $(^3\text{He},t)$ reactions, it was shown that the proportionality was valid for the transitions with $B(\text{GT}) \geq 0.04$ from the study of analogous transitions in $A=27$, $T=1/2$ mirror nuclei ^{27}Al and ^{27}Si [13].

It is known that the product $KN_{\sigma\tau}$ in Eq. (32) gradually changes as a function of excitation energy [5]. To estimate this effect, a distorted-wave Born approximation (DWBA) calculation was performed by using the code DW81 [38] and assuming a simple $d_{5/2} \rightarrow d_{3/2}$ transition for the excited GT states. As optical potential parameters, those determined for ^{28}Si at an incident ^3He energy of 150 MeV/nucleon [39] were used. For the outgoing triton channel, by following the arguments given in Ref. [40], the well depths were multiplied by a factor of 0.85 without changing the geometrical parameters of the optical potential. For the effective projectile-target interaction of the composite ^3He particle, the form derived by Schaeffer [41] through a folding procedure was used. Since the interaction strengths at 140 MeV/nucleon are not well studied, we tentatively used the value $V_{\sigma\tau} = -2.1$ MeV. The range $R = 1.415$ fm was derived by an extrapolation of the value that worked well at 67 MeV/nucleon [42]. The calculated 0° cross section decreased by about 11% as E_x increased up to 10 MeV. The result was used to correct the peak intensity of each state.

In order to obtain $B(\text{GT})$ values by using Eq. (32), a standard $B(\text{GT})$ value is needed. As a standard, we used the $B(\text{GT})$ value of 0.146 obtained in the β decay from the ^{23}Mg ground state to the 0.440 MeV state of ^{23}Na . Due to isospin symmetry of mirror nuclei, it is expected that the $B(\text{GT})$ values of mirror transitions are the same. We assumed that the transition to the 0.451 MeV state in ^{23}Mg has this $B(\text{GT})$ value in the $^{23}\text{Na}(^3\text{He},t)$ reaction. The $B(\text{GT})$ values for other excited states were calculated by using the proportionality [Eq. (32)] from their peak intensities after excitation-energy correction was made. The resulting $B(\text{GT})$ values are listed in column 7 of Table I and shown in Fig. 2(a) as a function of excitation energy.

As mentioned in the preceding subsection, both GT and Fermi transitions contribute incoherently in the transition between ground states. Since we cannot get the peak intensity for the Fermi transition corresponding to $B(\text{F}) = 1$ from the data available in the present analysis, the maximum $B(\text{GT})$ value assuming only the GT transition is tentatively given in Table I for this transition.

The $B(\text{GT})$ values were previously evaluated for the transitions to two low-lying states in a (p,n) reaction at $E_p = 160$ MeV [43]. The values were 0.153 and 0.062 for the 0.45 and 2.36 MeV states, respectively. In deriving these values, the authors assumed a universal unit cross section averaged over various nuclei. If these values are normalized

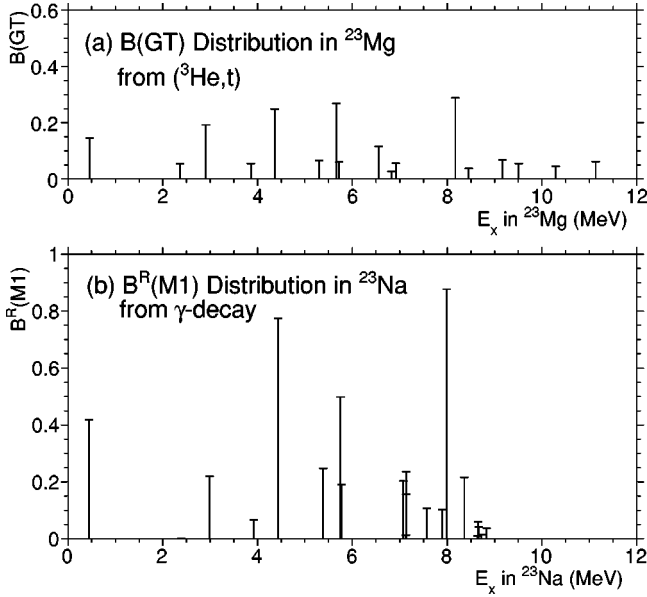


FIG. 2. Comparison of $B(\text{GT})$ and $B^R(M1)$ strength distributions. (a) $B(\text{GT})$ strength distribution from the present $^{23}\text{Na}(^3\text{He},t)^{23}\text{Mg}$ reaction. (b) $B^R(M1)$ strength distribution deduced from the γ -decay data. For the definition of $B^R(M1)$, see text.

by the above-mentioned β -decay $B(\text{GT})$ value that we used, then the $B(\text{GT})$ values would become 0.146 and 0.059, which are in agreement with our values of 0.146 and 0.055, respectively.

C. $M1$ γ -transition strength in ^{23}Na and ^{23}Mg

States with $J^\pi=1/2^+, 3/2^+$, and $5/2^+$ can decay directly to the $3/2^+$ ground state by $M1$ transitions. The $M1$ γ -transition strength $B(M1)\downarrow$ (in units of μ_N^2) from an excited state to the ground state of ^{23}Na is calculated using the measured lifetime (mean life) τ_m (in units of second), γ -ray branching ratio b_γ (in %) to the ground state, $E2$ and $M1$ mixing ratio δ , and the γ -ray energy E_γ (in MeV). The relationship among them is given (see, e.g., Ref. [3]) by

$$B(M1)\downarrow = \frac{1}{\tau_m} \frac{1}{E_\gamma^3} \frac{b_\gamma}{100} \frac{1}{1+\delta^2} \frac{1}{1.76 \times 10^{13}}. \quad (33)$$

It is expected that the γ -decay data are less reliable above the proton separation energy $S_p=8.79$ MeV in ^{23}Na . Therefore, the $B(M1)\downarrow$ values were calculated up to $\approx S_p$ region for all states that possibly have those three J^π values by using data compiled in Ref. [31] and the data from Refs. [44,45]. The $B(M1)\downarrow$ distribution, however, was far from being complete, because either lifetime and/or branching ratio were often missing for many states above $E_x=6$ MeV. Data of mixing ratios δ are not available for the states at $E_x=2.391, 4.430$, and 5.766 MeV and for all states above 7 MeV in ^{23}Na . For these states $\delta=0$, i.e., pure $M1$ transitions without mixing of $E2$, were assumed. The $B(M1)\downarrow$ values for these transitions should be considered upper bounds.

The $B(M1)\downarrow$ values were obtained only for the two low-lying states in ^{23}Mg . For the 2.359 MeV state, only the lifetime τ_m is known. Therefore the same branching ratio b_γ as for the analog state (2.391 MeV state) in ^{23}Na and $\delta=0$ are assumed.

In order to determine the $B(M1)\uparrow$ values that would be obtained in an (e, e') -type transition from the ground state with the spin value J_0 to the j th excited state with the spin value J_j , the $B(M1)\downarrow$ values from γ decays are modified by the $2J+1$ factors of the j th state and the ground state as

$$B(M1)\uparrow = \frac{2J_j+1}{2J_0+1} B(M1)\downarrow. \quad (34)$$

The $B(M1)\uparrow$ values for the excited states of ^{23}Na and ^{23}Mg are given in columns 4 and 6 of Table II, respectively. For the ground states of these nuclei, the values of magnetic moment μ from Ref. [46] and Ref. [47], respectively, are listed.

V. ANALOG STATES AND R VALUES

In order to compare the $B(M1)\uparrow$ values directly with the $B(\text{GT})$ values, we use $B^R(M1)$ values defined by Eqs. (15) and (16), respectively, for $T=1/2$ and $3/2$ states. The $B^R(M1)$ values for the $M1$ transitions in ^{23}Na are listed in column 3 of Table III and shown in Fig. 2(b).

Analog states in $T_0=1/2$ mirror nuclei should have similar and corresponding excitation energies. In addition, both $M1$ and GT transitions excite only $J^\pi=1/2^+, 3/2^+$, and $5/2^+$ states in the transitions from the $J^\pi=3/2^+$ ground state. By comparing the $B(\text{GT})$ and $B^R(M1)$ distributions shown in Figs. 2(a) and 2(b), respectively, corresponding ^{23}Mg and ^{23}Na states can be identified below $E_x=6$ MeV. The correspondence, however, is not clear above $E_x=6$ MeV. In Ref. [31], analog states in $A=23$ nuclei are compiled up to $E_x=6.6$ MeV. Based on this compilation and the correspondence of states seen in Fig. 2, pairs of analog states in ^{23}Na and ^{23}Mg are listed in the same row in Table III. Although GT states were clearly observed even above $E_x=8.8$ MeV in ^{23}Mg , the knowledge of an analogous relationship could not be extended to the region above 6 MeV. This is mainly due to insufficient γ -decay data, especially due to uncertain J^π values of higher excited states. In fact, in a similar comparison for the mirror pair ^{27}Al - ^{27}Si , a good correspondence of states was observed up to the S_p value [13].

There is a tendency that a state in ^{23}Mg is found at a lower excitation energy than the analog state in ^{23}Na . The difference of excitation energies ΔE_x , shown in column 5 of Table III, gradually increases with E_x .

From the comparison of Figs. 2(a) and 2(b) and also from the values listed in Table III, it is seen that the $B^R(M1)$ values of ^{23}Na states are much larger than $B(\text{GT})$ values of the analog states in ^{23}Mg for stronger transitions. On the other hand, for the 2.391–2.360 MeV pair, where both $B^R(M1)$ and $B(\text{GT})$ values are relatively small, $B^R(M1)$ is smaller. Similar $B^R(M1)$ and $B(\text{GT})$ values are observed for the 2.982–2.906 MeV and 3.914–3.860 MeV pairs. As we discussed in Sec. II A, $B^R(M1)$ and $B(\text{GT})$ values should be

TABLE II. States in ^{23}Na and ^{23}Mg , and the deduced $M1$ transition strengths $B(M1)\uparrow$ from the ground state to them. The $B(M1)\uparrow$ values were calculated from the γ -decay data compiled in Ref. [31]. The excitation energies are given in units of MeV. The $B(M1)\uparrow$ values are given in units of μ_N^2 . The isospin value $T=1/2$ is assumed unless $2T=3$ is specified.

E_x^a	States in ^{23}Na			E_x^a	States in ^{23}Mg
	$2J^\pi^a$	$2T^a$	$B(M1)\uparrow$		$B(M1)\uparrow$
0.0	3^+		2.218 ^b	0.0	-0.536 ^c
0.440	5^+		0.554 ± 0.034	0.451	0.591 ± 0.064
2.391	1^+		0.0017 ± 0.0003^d	2.359	0.0017 ± 0.0004^d
2.982	3^+		0.292 ± 0.041		
3.914	5^+		0.090 ± 0.015		
4.430	1^+		1.02 ± 0.07^d		
5.379	5^+		0.33 ± 0.12		
5.742	5^+		0.66 ± 0.04		
5.766	3^+		0.25 ± 0.04^d		
7.071	$(3-7^+)$		0.269 ± 0.024^d		
7.122	$(1-7^+)$		0.019 ± 0.007^d		
7.133	$(3,5)^+$		$\left\{ \begin{array}{l} 0.21 \pm 0.05^{d,e} \\ 0.31 \pm 0.07^{d,f} \end{array} \right.$		
7.566	$(5,7^+)$		0.14 ± 0.12^d		
7.891	5^+	3	0.130 ± 0.009^d		
7.991	$(1-7^+)$		1.16 ± 0.48^d		
8.360	(3^+-7^+)		0.29 ± 0.13^d		
8.631	$(3,5^+,7^+)$		0.015 ± 0.004^d		
8.646	$(1-7^+)$		0.079 ± 0.025^d		
8.664	1^+	(3)	0.054 ± 0.011^d		
8.721	$(1-7^+)$		0.020 ± 0.004^d		
8.830	1^+		0.050 ± 0.022^d		

^aFrom Ref. [31].

^bMagnetic moment μ from Ref. [46].

^cMagnetic moment μ from Ref. [47].

^dMaximum $B(M1)$ value, because mixing ratio $\delta=0$ is assumed.

^e $2J=3$ is assumed.

^f $2J=5$ is assumed.

similar under the assumption that the $\sigma\tau$ term in the $M1$ transition is dominant. In fact the similarity was observed for the transitions with $B(M1)\uparrow > 0.1$ for the mirror pair ^{27}Al - ^{27}Si [13]. In addition, we notice that $B^R(M1)$ values in ^{23}Na evaluated here are on average nearly one order of magnitude larger than those in ^{27}Al .

The enhancement of each $M1$ transition compared to the corresponding GT transition becomes clearer by looking at the ratios R_{ISO} . By using Eq. (17), the R_{ISO} values were calculated from $B^R(M1)$ and $B(\text{GT})$ values. Those values assuming $R_{\text{MEC}}=1.25$ are given in column 8 of Table III. The R_{ISO} values are also shown as a function of $B(M1)\uparrow$ in Fig. 3. It is observed that R_{ISO} values are large for strong transitions, suggesting that the combined IS and orbital contribution is large in stronger transitions. This was quite different in the ^{27}Al - ^{27}Si pair, where the R_{ISO} values became almost unity as the transition strength increased and $B(M1)\uparrow$ exceeded 0.1 (see Fig. 4 of Ref. [13]).

As examined in Sec. II A, the IV spin g factor g_s^{IV} is about an order of magnitude larger than other g factors. Therefore, if the reduced matrix element M for each term in Eq. (8) is of

average strength, it is expected that the IV spin term becomes larger than the other terms and that R_{ISO} has a value close to unity [1,13]. Obviously, this is not the case for some $M1$ transitions in ^{23}Na .

Since $B(M1)$ values of transitions to the ground state could be calculated only for two low-lying states in ^{23}Mg from the compilation of Ref. [31], the R_{IS} and R_{OC} values, which are calculated by using Eq. (23) and Eq. (24), respectively, are given only for these two pairs of states in Table IV. The R_{IS} and R_{OC} values can also be derived for the pair of ground states using the values of magnetic moments μ listed in Table II and the value of $B(\text{GT})=0.190$ from the β -decay measurement. We used Eq. (29) and Eq. (30) for calculating R_{IS} and R_{OC} , respectively.

It is interesting to see that the R_{IS} is almost unity for $M1$ transitions for the 0.440-0.451 MeV pair states, showing that the contribution of the isoscalar term is small. As a result, R_{OC} , showing the contribution of the isovector orbital ($l\tau$) term, is almost the same as R_{ISO} . A relatively small contribution of the isoscalar term was also observed in the analysis for the ^{27}Al - ^{27}Si pair [4]. It is therefore suggested that the

TABLE III. Analog states in ^{23}Na and ^{23}Mg and the $M1$ and the GT transition strengths. For details of the definition and derivation of $B^R(M1)$, see text. The ratio R_{ISO} showing the combined IS and orbital contributions in the $M1$ transition was calculated for each pair of analog states. Excitation energies are given in units of MeV.

E_x^a	States in ^{23}Na		E_x^b	ΔE_x	States in ^{23}Mg		R_{ISO} ($R_{\text{MEC}}=1.25$)
	$2J^\pi^a$	$B^R(M1)$			$2J^\pi^a$	$B(\text{GT})^b$	
0.440	5^+	0.419 ± 0.026	0.451	-0.011	5^+	0.146 ± 0.006^c	2.30 ± 0.17
2.391	1^+	0.0013 ± 0.0002^d	2.360	0.031	1^+	0.055 ± 0.004	0.019 ± 0.03
2.982	3^+	0.221 ± 0.031	2.906	0.076	$(3,5)^+$	0.193 ± 0.011	0.92 ± 0.14
3.914	5^+	0.068 ± 0.011	3.860	0.054	$(3,5)^+$	0.055 ± 0.004	0.99 ± 0.18
4.430	1^+	0.78 ± 0.05^d	4.357	0.073	1^+	0.250 ± 0.013	2.48 ± 0.22
5.379	5^+	0.25 ± 0.09	5.291	0.088	$(3,5)^+$	0.066 ± 0.005	3.0 ± 1.1
5.742	5^+	0.499 ± 0.031	5.658 ^e	0.084	5^+	0.270 ± 0.017	1.48 ± 0.13
5.766	3^+	0.191 ± 0.028^d	5.691 ^f		$(1-9)^+$		
			5.712 ^e		$(1-9)^+$	0.061 ± 0.009	
			6.550		$(1-9)^+$	0.116 ± 0.007	
			6.818			0.028 ± 0.003	
			6.911		5^+	0.057 ± 0.004	
7.071	$(3-7)^+$	0.203 ± 0.019^d					
7.122	$(1-7)^+$	0.014 ± 0.005^d					
7.133	{ $(3)^+$ $(5)^+$ }	{ $0.16 \pm 0.03^{d,g}$ $0.24 \pm 0.05^{d,h}$ }					
7.566	$(5,7)^+$	0.11 ± 0.09^d					
7.891	5^+	0.099 ± 0.007^d					
7.991	$(1-7)^+$	0.88 ± 0.37^d					
			8.168		5^+	0.290 ± 0.015	
8.360	(3^+-7^+)	0.22 ± 0.10^d					
			8.452		$(3-13)^+$	0.039 ± 0.003	
8.631	$(3,5^+,7^+)$	0.011 ± 0.003^d					
8.646	$(1-7)^+$	0.059 ± 0.019^d					
8.664	1^+	0.041 ± 0.009^d					
8.721	$(1-7)^+$	0.015 ± 0.003^d					
8.830	1^+	0.038 ± 0.016^d					
			9.159		$(3-13)^+$	0.069 ± 0.005	

^aFrom Ref. [31].

^bPresent work.

^cFrom β -decay experiment.

^dMaximum $B^R(M1)$ value, because mixing ratio $\delta=0$ is assumed.

^eClose doublet state.

^fExistence of this state is suggested in Ref. [31].

^g $2J=3$ is assumed.

^h $2J=5$ is assumed.

main part of the enhancement of $B(M1)$ values compared to the $B(\text{GT})$ values in several analogous transitions and therefore the large R_{ISO} values for them are due to large contributions of the $\ell\tau$ term in $M1$ transitions. We try to understand these findings in connection with the deformation of $A=23$ nuclei in the next section.

VI. DISCUSSION BASED ON NILSSON ORBITS AND PARTICLE-ROTOR MODEL

It is well known that in the middle of the sd shell, nuclei are largely deformed [14]. The static quadrupole moments Q_0 of ^{23}Na and ^{23}Mg are $10.1 \pm 0.2 \text{ fm}^2$ [48] and 11.4

$\pm 0.3 \text{ fm}^2$ [49], respectively. They are similar, and the large values suggest that these nuclei have a prolate deformation with a deformation parameter of $\delta \approx 0.5$. It has been discussed that the orbital contribution in the $M1$ transition can become large in deformed nuclei [50,51]. The contribution, however, is largely dependent on the configurations involved in the transitions.

We will first discuss the contributions of spin and orbital operators for the transitions between members of various rotational bands based on selection rules [52] assuming that each band is formed on a pure Nilsson orbit. Then we will analyze the observed spectra and different orbital contributions for $M1$ transitions.

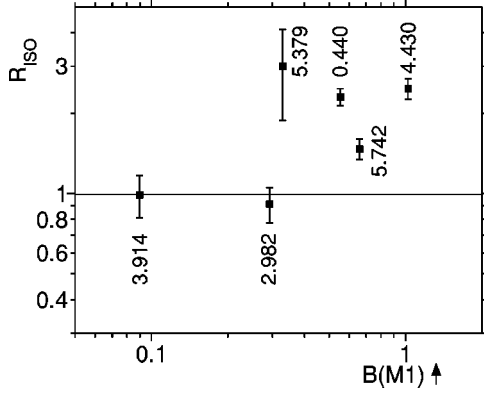


FIG. 3. The ratio R_{ISO} for $M1$ transitions in ^{23}Na . The ratio is sensitive to the combined contribution of IS term and IV orbital term to each $M1$ transition. Values of $R_{\text{ISO}} > 1$ (< 1) suggest constructive (destructive) interference of these terms with the IV spin term. For the definition of R_{ISO} , see text.

A. Spin and orbital contributions for $M1$ transitions among rotational bands

Let us consider an odd A , deformed nucleus with an even-even core. Under the assumption that the nucleus is symmetrical about the z axis, the single-particle orbits are labeled by using the asymptotic quantum numbers $[Nn_z\Lambda\Omega]$, where N is the total oscillator quantum number, n_z the number of quanta along the z axis, and Λ is the projection of the orbital angular momentum along the z axis. The projection of the total angular momentum of the single (odd) particle along the z axis is given by Ω . It is a good quantum number for a deformed field with axial symmetry [14]. By using the spin projection along the z axis $\Sigma (=s_z)$, Ω is expressed as $\Omega = \Lambda + \Sigma$. The low-lying spectra of odd- A deformed nuclei can be analyzed in terms of the intrinsic configuration, which is specified by the quantum numbers of the Nilsson orbit of the odd particle, with the rotational spectra. For axially symmetric intrinsic shape, the z component (K) of the total angular momentum J is a good quantum number. Since the z component of the rotational angular momentum of the axially symmetric core vanishes, $K = \Omega$ holds. Therefore, the values of total spin J are $J = K, K + 1, \dots$ for the band members.

1. Intraband transitions

In intraband transitions, asymptotic quantum numbers of intrinsic motion do not change. The matrix elements for the operators ℓ_z and σ_z are given by

$$\langle Nn_z\Lambda\Omega | \ell_z | Nn_z\Lambda\Omega \rangle = \Lambda \quad (35)$$

and

$$\langle Nn_z\Lambda\Omega | \sigma_z | Nn_z\Lambda\Omega \rangle = 2\Sigma, \quad (36)$$

respectively. Therefore both orbital and spin contributions are expected in the intraband $M1$ transitions. Since the orbital contribution is proportional to Λ , no orbital contribution is expected if the rotational band has $\Lambda = 0$. The phase relationship between the IV orbital term and the IV spin term are determined by the sign relationship of the values Λ and Σ , because both g_ℓ^{IV} and g_s^{IV} have positive sign. If the concerned single-particle Nilsson orbit originates from a so-called high j ($=\ell + 1/2$) type orbit in the spherical potential, like a $d_{5/2}$ orbit in the sd shell, then Λ and Σ have the same sign, and thus the orbital and the spin contributions are constructive. A similar constructive interference for a $j = \ell + 1/2$ orbit was discussed recently in Ref. [53]. Due to the selection rule $\Delta J = \pm 1$ (or 0), the intraband $M1$ transition is allowed only between neighboring members in the same rotational band.

2. Transitions caused by ℓ_\pm operator

Operators ℓ_\pm can cause transitions between states on different rotational bands. By applying ℓ_+ , we get

$$\ell_+ |Nn_z\Lambda\Omega\rangle \propto |Nn_z \pm 1 \Lambda + 1 \Omega + 1\rangle, \quad (37)$$

and by applying ℓ_- , we get

$$\ell_- |Nn_z\Lambda\Omega\rangle \propto |Nn_z \pm 1 \Lambda - 1 \Omega - 1\rangle, \quad (38)$$

where the relationship $0 \leq n_z \pm 1 \leq N$ and $0 \leq \Lambda \pm 1 \leq N$ should hold. Therefore ℓ_\pm connect the bands in which the asymptotic quantum numbers n_z and Λ change by one unit.

We use the above formulas (37) and (38) only for the IV orbital term of Eq. (8). It is expected that the contribution of the IS orbital term is very small in the formalism discussed in Sec. II A in which the odd particle is separated from the

TABLE IV. The $B_{\text{IS}}(M1)$ (μ_{IS}), $B_{\text{IV}}(M1)$ (μ_{IV}), R_{IS} , and R_{OC} values for the corresponding states in ^{23}Na and ^{23}Mg . For the definition of these values, see text. The excitation energies E_x are given in units of MeV. The values of $B_{\text{IS}}(M1)$ (μ_{IS}) and $B_{\text{IV}}(M1)$ (μ_{IV}) are given in units of μ_N^2 (μ_N).

E_x		$2J^\pi$	IS and IV terms		R_{IS}		R_{OC}
^{23}Na	^{23}Mg		$B_{\text{IS}}(M1)$	$B_{\text{IV}}(M1)$	^{23}Na	^{23}Mg	$R_{\text{MEC}} = 1.25$
0.0	0.0	3^+	0.841 ^a	1.377 ^b	2.59	0.15	2.3 ± 0.1
0.440	0.451	5^+	1×10^{-4}	0.57 ± 0.04	0.97 ± 0.07	1.03 ± 0.13	2.4 ± 0.2
2.391	2.359	1^+	1×10^{-8}	0.0017 ± 0.0003	1.0 ± 0.2	1.0 ± 0.2	0.019 ± 0.003^c

^aIS magnetic moment μ_{IS} .

^bIV magnetic moment μ_{IV} .

^cNot reliable, because of small IV spin term.

core-making collective rotation. The value of $g_\ell^{\text{IS}}=0.5-g_R$ almost vanishes, since the g factor of the rotor g_R is about 0.5 for $N=Z$ nuclei.

3. Transitions caused by σ_\pm operator

By applying σ_\pm , we get

$$\sigma_\pm |N n_z \Lambda \Omega\rangle \propto \delta(\Omega, \Lambda \mp 1/2) |N n_z \Lambda \Omega \pm 1\rangle. \quad (39)$$

As expected, σ_\pm cause transitions changing the asymptotic quantum number Σ , and thus Ω by one unit. It should be noted that both ℓ_\pm and σ_\pm operators cause interband transitions. They, however, connect bands with different characters.

The IS spin term is expected to be much smaller than the IV spin term. The value of $g_s^{\text{IS}}=0.880-g_R$ is almost 0.380, which becomes even smaller when one introduces a reduction factor for the proton and neutron spin g factors. We use the above formula (39) only for the IV spin term of Eq. (8).

4. Intensity ratios for transitions

Let us consider the $M1$ transitions starting from the band-head state of a rotational band K_1 to the members of a rotational band K_2 , assuming that the rotational perturbation of the intrinsic structure is negligible. Except for the case $K_1=K_2=1/2$, the $M1$ transition matrix element from a state $|J_1 K_1\rangle$ to a state $|J_2 K_2\rangle$ is reduced by using the intrinsic moments $\mathcal{M}(1, \nu)$ [see Eq. (4-91) of Ref. [14]] as

$$\begin{aligned} \langle J_2 K_2 || \mathcal{M}(1) || J_1 = K_1 K_1 \rangle \\ = \sqrt{2J_1 + 1} (J_1 K_1 1 K_2 - K_1 | J_2 K_2) \\ \times \langle K_2 | \mathcal{M}(1, \nu = K_2 - K_1) | K_1 \rangle, \end{aligned} \quad (40)$$

where J_2 can be J_1 or $J_1 \pm 1$. We see that $B(M1)$ values are proportional to the squared values of the CG coefficient $C_{\text{RB}}=(J_1 K_1 1 K_2 - K_1 | J_2 K_2)$ and the intrinsic moment $\mathcal{M}(1, \nu)$, where the latter value is independent of J_1 and J_2 and only dependent on the intrinsic structure. Therefore, transition strengths from a state with J_1 to the states with different J_2 are proportional to the squared values of C_{RB} , which are dependent on the value of J_2 .

If the transitions are of the type that were treated in Sec. VI A 2 or Sec. VI A 3, then the transitions are caused by the ℓ_\pm or σ_\pm operators. It should be noted that the relationship of Eq. (40) is valid even if the $M1$ operator $\mathcal{M}(1)$ is replaced by these operators. Since the σ_\pm operator is common to the GT operator, the proportionality to C_{RB}^2 is also extended to the analogous GT transitions.

B. Interpretation of the experimental results

It is known that the low-lying states of ^{23}Na form rotational bands based on Nilsson orbits mainly consisting of the proton $d_{5/2}$ wave function. The structure has been accounted for in a particle-rotor calculation including the effects of pair correlations [54]. By comparing the experimental data [31]

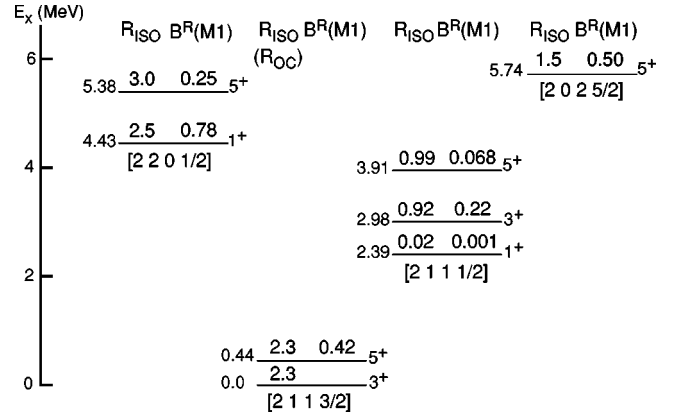


FIG. 4. Proposed band structure for the low-lying positive-parity states of ^{23}Na based on the Nilsson-orbit classification [54]. Each band is assigned by the combination of asymptotic quantum numbers $[N n_z \Lambda \Omega]$. The ratio R_{ISO} (for the ground state R_{OC}) and the $B^R(M1)$, which is proportional to $B(M1)^\dagger$, are also indicated. Each state is identified by the excitation energy (in MeV) and $2J^\pi$ value.

and the results of the calculation, a level scheme shown in Fig. 4 is proposed. In the figure, those states whose analog states are observed in the present $^{23}\text{Na}(^3\text{He}, t)^{23}\text{Mg}$ reaction are shown (see also Table III). Each state is identified by its excitation energy and $2J^\pi$ values. These are the states that can be connected directly to the ground state of ^{23}Na by $M1$ transitions. It was suggested that the ground state have almost pure $[2 1 1 3/2]$ nature with an amplitude of 0.99 [54].

In Ref. [54], the particle-rotor Hamiltonian was diagonalized, which contains a number of parameters such as moments of inertia, single-particle energies, pair-correlation parameters, and the reduction factor of the Coriolis force. Instead, in the present work, the data are analyzed in terms of Nilsson orbits of the odd particle and the related rotational bands. This simplified analysis may be justified, since we analyze only rotational states close to the respective band heads.

The values of R_{ISO} , showing the combined IS plus orbital contributions, and the transition strengths $B^R(M1)$ are indicated for each state in Fig. 4. We now try to understand these values based on the characteristics of transitions in deformed nuclei. As we have seen in the preceding subsection, largely different characteristics are expected depending on the different combinations of the initial and final deformed bands.

1. The ground-state band

The transition from the $J^\pi=3/2^+$ ground state to the 0.44 MeV, $5/2^+$ state is an intraband transition discussed in Sec. VI A 1, where the asymptotic quantum numbers $[2 1 1 3/2]$ are assigned for this band. Both ℓ and σ operators can contribute to the intraband transition. Since the major component of the $[2 1 1 3/2]$ orbit is $d_{5/2}$, a constructive interference is expected between the ℓ and σ contributions for this transition. A rather large experimental R_{ISO} value of 2.3 ($R_{\text{OC}}=2.4$) suggests a relatively large orbital contribution as a result of the constructive interference. The R_{IS} values were 0.97 and 1.03 in ^{23}Na and ^{23}Mg , respectively, which shows

that the IS term is about 1.5% of the IV term in the $M1$ matrix elements. These values near unity confirm the small IS contributions, as expected from the small g^{IS} values in Eq. (8).

The R_{OC} value of 2.3 obtained for the magnetic moment of the ground state is also consistent with the constructive interference of ℓ and σ contributions. If the ground and 0.44 MeV states form an ideal rotational band, the β -decay $B(\text{GT})$ values from the ^{23}Mg ground state to these states are expected to be proportional to the squared values of the CG coefficients C_{RB} in Eq. (40), as discussed in Sec. VI A 4. The C_{RB}^2 values are $(3/2\ 3/2\ 1\ 0|3/2\ 3/2)^2 = 3/5$ and $(3/2\ 3/2\ 1\ 0|5/2\ 3/2)^2 = 2/5$, respectively, for the transitions from a $J_1 = 3/2$ state to $J_2 = 3/2$ and $5/2$ states. Therefore a $B(\text{GT})$ ratio of 1.5 is expected. The experimental ratio of 1.3 calculated from Table I is in agreement, suggesting that this ground-state band is a good rotational band.

2. Transition to the $[2\ 2\ 0\ 1/2]$ band

The 4.43 MeV, $J^\pi = 1/2^+$ and the 5.38 MeV, $5/2^+$ states are assigned to be members of the $[2\ 2\ 0\ 1/2]$ band [54]. In the transitions from the ground state to these states, the asymptotic quantum number Λ decreases by one unit. As discussed in Sec. VI A 2, the transitions are mainly caused by the ℓ_- operator, and the contribution of the σ is only through the admixture of wave functions other than $[2\ 2\ 0\ 1/2]$. The R_{ISO} values are large for these transitions as seen in Fig. 4.

Under the assumption of the ideal rotational band with $K = 1/2$, the $M1$ transition strengths from the $J_1 = 3/2$ ground state to these states with $J_2 = 1/2$ and $5/2$ are proportional to C_{RB}^2 [Eq. (40)]. They are $(3/2\ 3/2\ 1 - 1|1/2\ 1/2)^2 = 0.5$ and $(3/2\ 3/2\ 1 - 1|5/2\ 1/2)^2 = 0.1$, respectively. Therefore a strength ratio of 5 is expected. In the measured transitions, the ratio is 3.1 as calculated from the $B^R(M1)$ values of these transitions shown in Fig. 4. It is suggested that the assumption of rotational band is good, but not ideal. The particle-rotor calculation [54] suggests some admixture of the $[2\ 0\ 2\ 5/2]$ configuration to the $J = 5/2$, 5.38 MeV state.

3. Transition to the $[2\ 1\ 1\ 1/2]$ band

Starting from the $J = 3/2$ ground state of the $[2\ 1\ 1\ 3/2]$ band, transitions to the $J = 1/2$, $3/2$, and $5/2$ members of the $[2\ 1\ 1\ 1/2]$ band are allowed. They are assigned to the states at 2.39, 2.98, and 3.91 MeV, respectively [54]. Due to the selectivity discussed in Sec. VI A 3, the transitions to these states are caused only by the σ_- operator under the assumption that asymptotic quantum numbers are valid. In addition, the transition strengths are expected to be proportional to C_{RB}^2 . They are 0.5, 0.4, and 0.1 for the J_2 values of $1/2$, $3/2$, and $5/2$, respectively.

For the transitions to the $J = 3/2$, 2.98 MeV and $J = 5/2$, 3.91 MeV states, the $B^R(M1)$ values are only slightly larger than the $B(\text{GT})$ values for the analogous transitions, and thus the obtained R_{ISO} , assuming $R_{\text{MEC}} = 1.25$, are nearly unity,

in agreement with the expectation that the transitions are caused mainly by the σ_- operator.

The ratio of $B^R(M1)$ values for the transitions to these states and also the ratio of $B(\text{GT})$ values for the analogous transitions are 3.3 and 3.5, respectively, as calculated from Table III. They are similar to the value of 4 expected from the squared ratio of CG coefficients C_{RB} relevant to these transitions.

The transition to the $J = 1/2$ band-head state shows a very small $B^R(M1)$ value, and the particle-rotor model calculation [54] fails to reproduce it. The corresponding $B(\text{GT})$ is also small, but not as small as $B^R(M1)$. The obtained R_{ISO} , therefore, is very small. In a shell-model calculation [55], it is suggested that a 20% admixture of the $[2\ 2\ 0\ 1/2]$ orbit to the $[2\ 1\ 1\ 1/2]$ wave function is needed to explain the weak transition strength.

4. Transition to the $[2\ 0\ 2\ 5/2]$ band

The $J = 5/2$, 5.74 MeV state in ^{23}Na is assigned to the band-head state of this rotational band [54], and its analog state is at $E_x = 5.66$ MeV in ^{23}Mg [31]. The $M1$ transition from the ground state is the second strongest in the low-lying region. Due to the $\Delta\Lambda = 1$ nature, the $M1$ transition from the ground state should be caused by the ℓ_+ operator. However, the obtained R_{ISO} value of 1.5 was not so large. It is suggested that some amount of contribution from the σ operator exists. The $B(\text{GT})$ value to the analog 5.66 MeV state in ^{23}Mg is actually large in the present analysis of the $^{23}\text{Na}(^3\text{He}, t)$ reaction, but some ambiguity exists. According to the compilation of Endt [31], the 5.691 MeV state in ^{23}Mg is the analog state of 5.766 MeV, $3/2^+$ state in ^{23}Na . We, however, could not resolve the 5.691 MeV state between 5.658 and 5.712 MeV states. As mentioned, peak decomposition assuming the three states was not successful. Therefore, it is still possible that the $B(\text{GT})$ value to the 5.66 MeV state in ^{23}Mg decreases and the R_{ISO} value increases, but on the basis of our finding, it is suggested that the $J = 5/2$, 5.74 MeV state is not an ideal member of the $[2\ 0\ 2\ 5/2]$ band. A resolution better than 20 keV would be needed for the CE reaction to make a definite statement.

VII. STATES OF ASTROPHYSICAL INTEREST

Because of its long half-life of 2.6 years, ^{22}Na is an important galactic γ emitter ($E_\gamma = 1.275$ MeV), where ^{22}Na is produced in the ‘‘hot’’ hydrogen-burning Ne-Na cycle, e.g., in nova explosions [56]. Since the abundance of ^{22}Na critically depends on the rate of $^{22}\text{Na}(p, \gamma)^{23}\text{Mg}$, the excitation energies of ‘‘resonance states’’ in ^{23}Mg situated slightly above the proton separation energy ($S_p = 7579.5 \pm 1.3$ keV [57]) are significant parameters. These ‘‘resonance states’’ and reaction rates have been studied in $^{25}\text{Mg}(p, t)$ [58], $^{24}\text{Mg}(p, d)$ [59], and $^{22}\text{Na}(^3\text{He}, d)$ [60] reactions as well as directly in $^{22}\text{Na}(p, \gamma)$ [61].

Since those states are not necessarily connected to the ground state of ^{23}Na with $L = 0$ transitions, they are not strongly populated in the small-angle spectrum shown in Fig. 1. Some of them, however, are clearly observed in the spec-

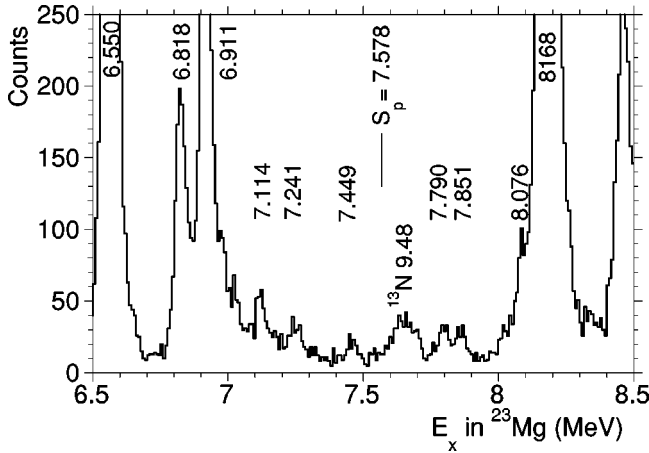


FIG. 5. The 6.5–8.5 MeV region of the $^{23}\text{Na}(^3\text{He},t)$ spectrum. Many $L \neq 0$ states are observed by analyzing events for almost full acceptance of the spectrometer. Excitation energies are given in units of MeV.

trum with a large angle cut (θ up to ± 20 mrad, ϕ up to about ± 40 mrad) as shown in Fig. 5.

Owing to the good energy resolution, accurate excitation energies are determined for these states. They are listed in Table V and compared with the previous values. We see that the present excitation energies that are determined independently are consistent with previous values.

VIII. SUMMARY

Assuming a mirror symmetry structure of the ^{23}Na - ^{23}Mg nuclei, the strengths of analogous $M1$ and GT transitions from the ground state of ^{23}Na were compared and examined. It is known that both nuclei are deformed, and their low-lying states are interpreted in terms of Nilsson orbits. Various properties inherent in the transitions among different deformed bands were identified.

The GT transitions were studied in the $^{23}\text{Na}(^3\text{He},t)^{23}\text{Mg}$ reaction at the intermediate incident energy of 140 MeV/nucleon. Owing to the 45 keV resolution, states up to $E_x = 11$ MeV of ^{23}Mg were clearly separated. The $\Delta E/E = 10^{-4}$ resolution achieved here is based on the successful implementation of dispersion matching between the spectrometer and the beam line, and also on the newly developed method of making a thin (≈ 2 mg/cm 2) ^{23}Na target.

The $B(GT)$ values in the $(^3\text{He},t)$ reaction were calibrated by using the $B(GT)$ value derived from a GT β decay of ^{23}Mg to the 0.440 MeV state in ^{23}Na , which is analogous to the transition from the ground state of ^{23}Na to the 0.451 MeV state of ^{23}Mg . Using the proportionality between the cross sections and the $B(GT)$ values in the 0° , $(^3\text{He},t)$ reaction at 140 MeV/nucleon, the $B(GT)$ values are obtained reliably for higher excited states. A DWBA calculation was used to correct for the excitation energy dependence of the cross section.

TABLE V. Excitation energies for ^{23}Mg states above the proton threshold. Excitation energies and their errors given in parentheses are shown in units of keV.

This work	$^{25}\text{Mg}(p,t)$ ^a	$^{24}\text{Mg}(p,d)$ ^b	$^{22}\text{Na}(^3\text{He},d)$ ^c	$^{22}\text{Na}(p,\gamma)$ ^d
	7780 (6)	7782	7780 (6)	7785 (3)
7790 (6)	7795 (6)		7795 (6)	
7851 (6)	7852 (6)	7856	7853 (4)	7855 (3)
	8016 (6)	8014	8016 (6)	
	8058 (6)	8055	8058 (7)	
8076 (15)	8076 (8)	8072	8076 (8)	
8168 (4)				8165 (3)

^aFrom Ref. [58].

^bFrom Ref. [59].

^cFrom Ref. [60].

^dFrom Ref. [61].

The strengths of analogous $M1$ and GT transitions were compared in terms of the deviation of R_{ISO} from unity, which mainly shows the contribution of the orbital part of the $M1$ operator. A large variety of values were observed for the ratio R_{ISO} depending on the nature of transitions characterized by different combinations of initial and final deformed bands. It was found that R_{ISO} values were large for an intraband transition and also for interband transitions in which the asymptotic quantum number Λ changes. On the other hand, for interband transitions in which the asymptotic quantum number Σ changes, R_{ISO} values of about unity were observed. The identification of one-particle orbits in deformed potential expressed in terms of asymptotic quantum numbers and the rotational bands formed on them was very useful for the interpretation of transition properties of low-lying states up to 5.7 MeV.

The high resolution of the spectrum allowed us to determine the level energies of excited states accurately even for weakly populated states. Excitation energies determined for the states above the proton threshold were in good agreement with those from other works. They play important roles as the “resonance states” in the $^{22}\text{Na}(p,\gamma)$ reaction of the “hot” hydrogen-burning Ne-Na cycle. This demonstrates the sensitivity that can be reached with the high resolution of the present $(^3\text{He},t)$ experiment.

ACKNOWLEDGMENTS

The $^{23}\text{Na}(^3\text{He},t)^{23}\text{Mg}$ experiment was performed at RCNP, Osaka University under the Experimental Program E158. The authors are grateful to the accelerator group of RCNP, especially to Professor T. Saito and Dr. S. Ninomiya, for their efforts in providing a high-quality ^3He beam indispensable for the realization of dispersion matching to achieve good energy resolution.

- [1] E. K. Warburton and J. Weneser, in *Isospin in Nuclear Physics*, edited by D.H. Wilkinson (North-Holland, Amsterdam, 1969), Chap. 5, and references therein.
- [2] S. S. Hanna, in *Isospin in Nuclear Physics*, edited by D.H. Wilkinson (North-Holland, Amsterdam, 1969), Chap. 12, and references therein.
- [3] H. Morinaga and T. Yamazaki, *In Beam Gamma-Ray Spectroscopy* (North-Holland, Amsterdam, 1976), and references therein.
- [4] Y. Fujita, B.A. Brown, H. Ejiri, K. Katori, S. Mizutori, and H. Ueno, *Phys. Rev. C* **62**, 044314 (2000), and references therein.
- [5] T.N. Taddeucci, C.A. Goulding, T.A. Carey, R.C. Byrd, C.D. Goodman, C. Gaarde, J. Larsen, D. Horen, J. Rapaport, and E. Sugarbaker, *Nucl. Phys.* **A469**, 125 (1987), and references therein.
- [6] C.D. Goodman, C.A. Goulding, M.B. Greenfield, J. Rapaport, D.E. Bainum, C.C. Foster, W.G. Love, and F. Petrovich, *Phys. Rev. Lett.* **44**, 1755 (1980).
- [7] J. Rapaport and E. Sugarbaker, *Annu. Rev. Nucl. Part. Sci.* **44**, 109 (1994).
- [8] B.D. Anderson, T. Chittarakarn, A.R. Baldwin, C. Lebo, R. Madey, P.C. Tandy, J.W. Watson, C.C. Foster, B.A. Brown, and B.H. Wildenthal, *Phys. Rev. C* **36**, 2195 (1987).
- [9] Y. Fujita *et al.*, *Phys. Rev. C* **55**, 1137 (1997).
- [10] Y. Fujita *et al.*, *Nucl. Instrum. Methods Phys. Res. A* **402**, 371 (1998).
- [11] Y. Fujita *et al.*, *Nucl. Phys.* **A690**, 243c (2001).
- [12] Y. Fujita *et al.*, *Nucl. Phys.* **A687**, 311c (2001).
- [13] Y. Fujita *et al.*, *Phys. Rev. C* **59**, 90 (1999).
- [14] A. Bohr and B. Mottelson, *Nuclear Structure II* (Benjamin, New York, 1969), and references therein.
- [15] A. Arima, K. Shimizu, and W. Bentz, in *Advances in Nuclear Physics*, edited by J. W. Negele and E. Vogt (Plenum, New York, 1987), Vol. 18, p. 1, and references therein.
- [16] I.S. Towner, *Phys. Rep.* **155**, 263 (1987).
- [17] A. Richter, A. Weiss, O. Häusser, and B.A. Brown, *Phys. Rev. Lett.* **65**, 2519 (1990).
- [18] C. Lüttge, P. von Neumann-Cosel, F. Neumeyer, C. Rangacharyulu, A. Richter, G. Schrieder, E. Spamer, D.I. Sober, S.K. Matthews, and B.A. Brown, *Phys. Rev. C* **53**, 127 (1996).
- [19] P. von Neumann-Cosel, A. Richter, Y. Fujita, and B.D. Anderson, *Phys. Rev. C* **55**, 532 (1997).
- [20] J. Rapaport and E. Sugarbaker, *Annu. Rev. Nucl. Part. Sci.* **44**, 109 (1994).
- [21] W.G. Love and M.A. Franey, *Phys. Rev. C* **24**, 1073 (1981).
- [22] M. Fujiwara *et al.*, *Nucl. Instrum. Methods Phys. Res. A* **422**, 484 (1999).
- [23] Y. Shimbara *et al.*, RCNP (Osaka Univ.), Annual Report, 2001; *Nucl. Instrum. Meth. Phys. Res. A* (to be published).
- [24] T. Noro *et al.*, RCNP (Osaka Univ.), Annual Report, 1991, p. 177.
- [25] Y. Fujita, K. Hatanaka, G.P.A. Berg, K. Hosono, N. Matsuoka, S. Morinobu, T. Noro, M. Sato, K. Tamura, and H. Ueno, *Nucl. Instrum. Methods Phys. Res. B* **126**, 274 (1997), and references therein.
- [26] T. Wakasa *et al.*, *Nucl. Instrum. Methods Phys. Res. A* **482**, 79 (2002).
- [27] H. Fujita *et al.*, *Nucl. Instrum. Methods Phys. Res. A* **484**, 17 (2002).
- [28] Y. Fujita *et al.*, *J. Mass Spectrom. Soc. Jpn.* **48**, 306 (2000).
- [29] H. Fujita *et al.*, *Nucl. Instrum. Methods Phys. Res. A* **469**, 55 (2001).
- [30] X. Wang *et al.*, *Phys. Rev. C* **63**, 024608 (2001).
- [31] P.M. Endt, *Nucl. Phys.* **A521**, 1 (1990); **A633**, 1 (1998), and references therein.
- [32] F. Ajzenberg-Selove, *Nucl. Phys.* **A523**, 1 (1991).
- [33] D.R. Tilley, H.R. Weller, and C.M. Cheves, *Nucl. Phys.* **A564**, 1 (1993).
- [34] I. Towner, E. Hagberg, J. C. Hardy, V. T. Koslowsky, and G. Savard, in *Proceedings of the International Conference on the Exotic Nuclei and Atomic Masses*, ENAM95, Arles, 1995, edited by M. de Saint Simon and O. Sorlin (Editions Frontieres, Gif-sur-Yvette, 1996), p. 711; I. Towner (private communication).
- [35] D.H. Wilkinson and B.E.F. Macefield, *Nucl. Phys.* **A232**, 58 (1974).
- [36] K. Schreckenbach, P. Liaud, R. Kossakowski, H. Nastoll, A. Bussiere, and J.P. Guillaud, *Phys. Lett. B* **349**, 427 (1995).
- [37] W.G. Love, K. Nakayama, and M.A. Franey, *Phys. Rev. Lett.* **59**, 1401 (1987).
- [38] DW81, a DWBA computer code by J. R. Comfort (1981) and updated version (1986), an extended version of DWBA70 by R. Schaeffer and J. Raynal (1970).
- [39] T. Yamagata *et al.*, *Nucl. Phys.* **A589**, 425 (1995).
- [40] S.Y. van der Werf, S. Brandenburg, P. Grasdijk, W.A. Sterrenburg, M.N. Harakeh, M.B. Greenfield, B.A. Brown, and M. Fujiwara, *Nucl. Phys.* **A496**, 305 (1989).
- [41] R. Schaeffer, *Nucl. Phys.* **A164**, 145 (1971).
- [42] S. Y van der Werf and R. G. T. Zegers (private communication).
- [43] C. D. Goodman, in *Proceedings of the International Symposium on the Nuclear Reaction Dynamics of Nucleon-Hadron Many Body System*, Osaka, 1995, edited by H. Ejiri, T. Noro, K. Takahisa, and H. Toki (World Scientific, Singapore, 1996), p. 125.
- [44] E.L. Bakkum and C. Van der Leun, *Nucl. Phys.* **A500**, 1 (1989).
- [45] P. Tikkanen, J. Keinonen, K. Arstila, A. Kuronen, and B.H. Wildenthal, *Phys. Rev. C* **42**, 581 (1990).
- [46] P. Raghavan, *At. Data Nucl. Data Tables* **42**, 189 (1989).
- [47] M. Fukuda, T. Izumikawa, T. Ohtsubo, M. Tanigaki, S. Fukuda, Y. Nakayama, K. Matsuta, Y. Nojiri, and T. Minamisono, *Phys. Lett. B* **307**, 278 (1993).
- [48] B. Jeckelmann, W. Beer, I. Beltrami, F.W.N. De Boer, G. De Chambrier, P.F.A. Goudsmit, J. Kern, H.J. Leisi, W. Ruckstuhl, and A. Vacchi, *Nucl. Phys.* **A408**, 495 (1983); P. Raghavan, *At. Data Nucl. Data Tables* **42**, 189 (1989).
- [49] K. Matsuta *et al.*, *Hyperfine Interact.* **120/121**, 673 (1999).
- [50] D. Bes and R. Broglia, *Phys. Lett.* **137B**, 141 (1984).
- [51] I. Hamamoto and W. Nazarewicz, *Phys. Lett. B* **297**, 25 (1992).
- [52] J.P. Boisson and R. Piepenbring, *Nucl. Phys.* **A168**, 385 (1971).
- [53] A.F. Lisetskiy, A. Gelberg, R.V. Jolos, N. Pietralla, and P. von Brentano, *Phys. Lett. B* **512**, 290 (2001).
- [54] M. Guttormsen, T. Pedersen, J. Rekestad, T. Engeland, E. Osnes, and F. Ingebretsen, *Nucl. Phys.* **A338**, 141 (1980).

- [55] B.J. Cole, A. Watt, and R.R. Whitehead, Phys. Lett. **55B**, 11 (1975).
- [56] J. José, A. Coc, and M. Hernanz, Astrophys. J. **520**, 347 (1999).
- [57] G. Audi and A.H. Wapstra, Nucl. Phys. **A565**, 1 (1993).
- [58] H. Nann, A. Saha, and B.H. Wildenthal, Phys. Rev. C **23**, 606 (1981).
- [59] S. Kubono *et al.*, Z. Phys. A **348**, 59 (1994).
- [60] S. Schmidt, C. Rolfs, W.H. Schulte, H.P. Trautvetter, R.W. Kavanagh, C. Hategan, S. Faber, B.D. Valnion, and G. Graw, Nucl. Phys. **A591**, 227 (1995).
- [61] S. Seuthe *et al.*, Nucl. Phys. **A514**, 471 (1990); F. Stegmüller, C. Rolfs, S. Schmidt, W.H. Schulte, H.P. Trautvetter, and R.W. Kavanagh, *ibid.* **A601**, 168 (1996).